

Chapter 2

Theoretical Background

In this chapter, we discuss the literature survey of retinal blood vessels segmentation and registration, performance measures used to evaluate the performance of segmentation and registration approach, and describe the database used during the segmentation and registration process.

2.1 Introduction

Retinal vessel segmentation is a prominent task for the diagnosis, screening, treatment, and evaluation of various cardiovascular and ophthalmic diseases such as diabetes, hypertension, arteriosclerosis and cordial neovascularization [16]. Automatic retinal blood vessels segmentation and analysis can assist in the implementation of screening programs for diabetic retinopathy [17], evaluation of retinopathy of pre-maturity [18], arteriolar narrowing [19], the relationship between vessel tortuosity and hypertensive retinopathy [19], foveal avascular region detection [20], vessel diameter measurement in relation with diagnosis of hypertension [21], and computerized laser surgery [16]. Automatic generation of retinal maps and extraction of branch points have been used for multi modal or temporal image registration [22], and retinal image mosaic analysis [23]. Moreover, the retinal vessels structure is also used for biometric identification [24],[25] because it must be unique for each individual except in case of pathology.

This literature survey, particularly focuses on the various approaches used for seg-

mentation of retinal blood vessels from two dimensional colored retinal images captured by a fundus camera. The main objectives of this survey are to review the retinal vessel segmentation approaches; Discussion about the databases used for retinal image segmentation, to provide a detailed description of the approaches used for vessel segmentation and also discuss the merits and demerits of the various approaches; to discuss the current trends and future directions and summarize the open problems. This chapter also focused on the challenges related to the retinal image segmentation.

2.2 Classification of retinal blood vessels segmentation approaches: A review

According to author M. M. Fraz *et al.* [6] the retinal blood vessel segmentation approaches are mainly classified into seven categories, namely, the intensity based pattern recognition techniques, mathematical morphology based, vessel tracking based, model based, parallel hardware based, multi-scale based techniques and matched filter based approach.

2.2.1 Intensity based pattern recognition approach

The intensity based pattern recognition techniques, handles the automatic retinal blood vessel detection or classification from their background and they are divided into two categories, namely supervised approaches [26, 27, 28] and unsupervised approaches [29, 30]. The supervised approaches are based on some prior labeling information which are used to decide whether a pixel belongs to a retinal blood vessel or non-retinal blood vessel, whereas the unsupervised techniques perform the vessel segmentation without any prior labeling information.

2.2.1.1 Supervised Approach

In a supervised method, the classification criteria are determined by the ground truth data based on known features. Therefore the prerequisite is the availability of already classified

ground truth data, which may not be available in real life applications. The supervised methods of retinal blood vessel segmentation are based on pre-classified data, hence the performance is usually better than that of unsupervised ones and can produce very good results for healthy retinal images. Many authors work on supervised classification based retinal blood vessel segmentation.

2.2.1.2 Unsupervised Approach

The approach based on unsupervised classification attempt to find inherent patterns of blood vessels in retinal images that can then be used to determine that a particular pixel belongs to vessel or not. The training data or hand labeled ground truths do not contribute directly to the design of the algorithm in these approaches.

2.2.2 Mathematical morphology based Approach

The mathematical morphology is a tool used for extracting the image components. The extracted components are used to describe the features, boundaries, convex hulls and skeletons. The mathematical morphology provides a unique and powerful approach for image processing. Morphological image processing [31] is based on morphological operators which is normally applied to the binary image by using Structuring Elements (SE) and it can be extended for gray scale image. Dilation and erosion are main morphological operators, where the dilation is used to expand the object, and the erosion is used for thinning the object with the help of SE. There are two other morphological operators which are derived from dilation and erosion namely opening and closing operation. The top-hat [32] and watershed [33] transformation algorithms are related to mathematical morphology. The top-hat algorithm extracts the low contrast elements and details of the given image and they are divided into two categories, namely white top-hat and black top-hat algorithms. The white top-hat and black top-hat algorithms are defined as the difference between the input image and its opening and closing respectively by using some SE. The top-hat algorithm is used for retinal blood vessel extraction because the retinal blood vessels have comparatively low contrast in comparison to their background. The

watershed transformation algorithm is also used for medical image segmentation by using mathematical morphology tools with Gaussian shape structures, but it was observed that it may give reasonable results with retinal images. The basic morphology of the vessels structure is known a priori to be comprised of connected linear segments. Morphological processing for identifying specific shapes has the advantage of speed and noise resistance. The main disadvantage of exclusively relying upon morphological approaches is that they do not exploit the known vessel cross-sectional shape. In addition, the use of an overly long structuring element may cause difficulty in fitting to highly tortuous vessels.

2.2.3 Model-based approach

The Model-based approaches are applied for extracting the vessel's structure of the retinal image. This approach is classified into two categories, namely deformable model and vessel profile model.

2.2.3.1 Deformable model

The deformable model for vessel extraction is further classified into two categories, namely a geometric deformable model and a parametric deformable model. The geometric deformable model is based on the theory of curve evolution geometric flow and implemented by using level set based numerical technique. This numerical technique is used for tracking shapes and interfaces of vessels and the main advantage is that, it can be performed on a fixed Cartesian grid without parameterizing the objects.

The parametric deformable model is also known as a snake model [34, 35]. Snakes are the curves defined within an image that can move under the influence of internal forces within the curve itself and external forces derived from the image data. These internal and external are responsible to identify the boundary of the objects and other inside features of the image. The internal forces are also known as smoothing and they produce the tension and stiffness which control the behavior of the deformation, whereas the external forces can be specified by human or supervising process. The advantages of snakes are that they are autonomous and self-adapting in their search for a minimal energy state.

2.2.3.2 Vessel intensity profile model

The intensity profile of the vessel cross section is normally an approximate Gaussian shape but there exists some other shapes of intensity profiles of the vessel cross section in literature such as cubic spline, the second-order derivative Gaussian etc. The more complex scenario is to include the non-vessel features like bright or dark lesions and the background characteristic in the vessel detection model to increase the segmentation accuracy in difficult imaging conditions. The flat background has also been assumed in some profile models for the vessel section. Vessel crossing and branching can further complicate the profile model.

The existing approach in literature focuses on the vessel intensity profile. Author Vermeer *et al.* [36] proposed the vessel profile model as Laplacian that incorporate the central vessel reflex. Wang *et al.* [37] proposed a multi-resolution Hermite model for vascular segmentation by using two-dimensional Hermite function intensity model. Mahadevan *et al.* [38] proposed modular framework for vessel detection in noisy retinal images whereas the author Lam *et al.* [39] proposed a segmentation algorithm for pathological retinal images which is based on the divergence of vector fields and further proposed in Lam *et al.* [40], a regularization based multi-concavity model which is able to segment both the pathological as well as normal retinal images.

2.2.4 Vessel tracking based approach

The vessel tracking based approach segments the retinal blood vessels between two points rather than the entire vascular structure. The initial set of points is established automatically by using their local information or by manually. The center of the vessel cross-section is determined by using some characteristic of the blood vessels such as gray level intensity, average width and tortuosity measured during tracking. Tracking consists of vessel center lines according to their local information, and try to find the most appropriate path, which best matches to the vessel profile model. The tracking based approach provides accurate width and the information of individual blood vessels that is normally not provided by other approaches. This approach also provides some information about

the blood vessel structures such as branching and the connectivity. The main disadvantage of this approach is that it cannot detect the blood vessel and their segments which have no seed points and if any bifurcation points are missing then the respective sub-trees remains undetected.

2.2.5 Parallel hardware based approach

The parallel hardware based implementation of retinal blood vessel segmentation algorithm reduces the computational cost of segmentation algorithm and provide better real-time performance. A typical example for real-time image processing is cellular neural network [41, 42] and implemented at Very Large Scale Integrated Circuit (VLSI). In case of high resolution images, the parallel vessel segmentation algorithms are implemented by using segmentation and registration Toolkit [43]. The Toolkit have been implemented in C++ programming language and also wrapped for Python, Java and Tcl. This Toolkit provides the segmentation and registration algorithms for two dimensions as well as multi dimensions.

2.2.6 Multi-scale based approach

In the retinal image when one visually observe the blood vessels then it is found that the width of blood vessel continuously decreases, when it moves radially away from the optical disk of retinal image. It is also observed that the retinal blood vessels are in low contrast pattern having a Gaussian shape cross-section profile locally linear in nature, piecewise connected and gradually decreasing width. So the basic idea behind multi-scale approach is to separate out the information related to the retinal blood vessels according to various levels of their width at different scales.

2.2.7 Matched filter based approach

Matched filtering approach for the segmentation of the retinal blood vessel structure convolves a 2-D kernel with the retinal image. The kernel is designed to model a feature in the image at some unknown position and orientation, and the Matched Filter Response

(MFR) indicates the presence of the feature. There are three properties which are important to design the matched filter kernel:

- Retinal blood vessels have a limited curvature and may be approximated by piecewise linear segments.
- The diameter of retinal blood vessels decrease as they move radially outward from the optic disk.
- The cross-sectional intensity profile of line segment.

The convolution kernel may be quite large and needs to be applied at several rotations resulting in a computational overhead. In addition, the kernel responds optimally to vessels that have the same standard deviation of the underlying Gaussian function specified by the kernel. As a consequence, the kernel may not respond to those vessels which have a different profile. The retinal background variation and presence of pathologies in the retinal image also increase the number of false responses because the pathologies can exhibit the same local attributes as the vessels. A matched filter response method is found more effective with other retinal image segmentation approach.

First time Chaudhuri *et al.* [12] in 1989, compare the intensity level of the cross-section profile of the retinal image with Gaussian curve and stated that the cross-sectional profile of retinal blood vessels has an approximate Gaussian shape and proposed a Gaussian shaped matched filter based approach to segment the retinal blood vessels. After that various authors Al-Rawi *et al.* [13], Xiaoyi and Mojon [44], Cinsdikici *et al.* [45], and Amin and Yan [46] improved the performance of matched filter based approach by improving the thresholding techniques rather than changing the Gaussian shaped matched filter kernel. In 2010 author Zhang *et al.* [47] proposed a matched filter approach with first-order derivative of Gaussian and improve the performance but this approach is the combination of the classical matched filter, which is a zero-mean Gaussian function, and the first-order derivative of Gaussian. In 2014 author H. Zolfagharnasa *et al.* [14] first time replace the Gaussian function based matched filter by Cauchy probability distribution function (pdf) and reported that the accuracy of retinal blood vessel detection was

substantially improved.

Category wise performance measures of various retinal blood vessel segmentation approaches based on DRIVE database and STARE database are mentioned in Table 2.1 and Table 2.2 respectively.

Table 2.1: Performance measures of various retinal blood vessel segmentation approaches based on DRIVE database

Author's name	TPR	FPR	Accuracy	Category
Human observer	0.7763	0.02770	0.9470	
Abramoff <i>et al.</i> [27]	0.7145	—	0.9416	Supervised
Staal <i>et al.</i> [26]	—	—	0.9442	Supervised
Soares <i>et al.</i> [48]	—	—	0.9466	Supervised
Ricci <i>et al.</i> [49]	—	—	0.9563	Supervised
Lupascu <i>et al.</i> [50]	0.7200	—	0.9597	Supervised
Xu and Luo [51]	0.7760	—	0.9328	Supervised
You <i>et al.</i> [52]	0.7410	0.0249	0.9434	Supervised
Marin <i>et al.</i> [53]	0.7067	0.0199	0.9452	Supervised
Kande <i>et al.</i> [54]	—	—	0.8911	Unsupervised
Zana and Klein [55]	0.6971	—	0.9377	Morphological
Mendonca <i>et al.</i> [56]	0.7344	0.0236	0.9452	Morphological
Fraz <i>et al.</i> [57]	0.7152	0.0231	0.9430	Morphological
Miri and Mahloojifar [58]	0.7352	0.0205	0.9458	Morphological
Li <i>et al.</i> [37]	0.7800	0.0220	—	Model-based
Lam <i>et al.</i> [40]	—	—	0.9472	Model-based
Espona <i>et al.</i> [35]	0.6634	0.0318	0.9316	Model-based
Espona <i>et al.</i> [59]	0.7436	0.0385	0.9352	Model-based
Al-Diri <i>et al.</i> [60]	0.7282	0.0449	—	Model-based
Zhang <i>et al.</i> [61]	—	0.0228	0.9610	Model-based
Renzo <i>et al.</i> [62]	—	—	0.9348	Parallel hardware
Alonso-Montes [63]			0.9185	Parallel hardware
Palomera-Perez <i>et al.</i> [64]	0.6400	0.0330	0.9250	Parallel hardware
Martinez-Perez <i>et al.</i> [65]	0.6389	—	0.9181	Multiscale
Martinez-Perez <i>et al.</i> [66]	0.7246	0.0345	0.9344	Multiscale
Perez <i>et al.</i> [67]	0.6600	0.0388	0.9220	Multiscale
Anzalone <i>et al.</i> [68]	—	—	0.9419	Multiscale
Vlachos and Dermatas [69]	0.7470	0.0450	0.9290	Multiscale
Chaudhuri <i>et al.</i> [12]	—	—	0.8773	Matched filter
Xiaoyi and Mojon [44]	—	—	0.9212	Matched filter
Al-Rawi <i>et al.</i> [13]	—	—	0.9535	Matched filter
Zhang <i>et al.</i> [47]	0.7120	0.0276	0.9382	Matched filter
Cinsdikici <i>et al.</i> [45]	—	—	0.9293	Matched filter
Amin and Yan [46]	—	—	0.9200	Matched filter
H. Zolfagharnasa <i>et al.</i> [14]	0.6239	0.0286	0.9269	Matched filter

Table 2.2: Performance measures of various retinal blood vessel segmentation approaches based on STARE database

Author's name	TPR	FPR	Accuracy	Category
Human observer	0.8951	0.0616	0.9348	
Staal <i>et al.</i> [26]	—	—	0.9516	Supervised
Soares <i>et al.</i> [48]	—	—	0.9480	Supervised
Ricci <i>et al.</i> [49]	—	—	0.9584	Supervised
You <i>et al.</i> [52]	0.7260	0.0244	0.9497	Supervised
Marin <i>et al.</i> [53]	0.6944	0.0181	0.9526	Supervised
Kande <i>et al.</i> [54]	—	—	0.8976	Unsupervised
Salem <i>et al.</i> [70]	0.8215	0.0250	—	Unsupervised
Mendonca <i>et al.</i> [56]	0.6996	0.0270	0.9440	Morphological
Fraz <i>et al.</i> [57]	0.7311	0.0320	0.9442	Morphological
Vermeer <i>et al.</i> [36]	—	—	0.9287	Model-based
Lam and Hong [39]	—	—	0.9474	Model-based
Li <i>et al.</i> [37]	0.7520	0.0200	—	Model-based
Lam <i>et al.</i> [40]	—	—	0.9567	Model-based
Al-Diri <i>et al.</i> [60]	0.7521	0.0391	—	Model-based
Zhang <i>et al.</i> [61]	0.7373	0.0264	0.9087	Model-based
Palomera-Perez <i>et al.</i> [64]	0.7690	0.0551	0.9260	Parallel hardware
Martinez-Perez <i>et al.</i> [66]	0.7506	0.0431	0.9410	Multiscale
Perez <i>et al.</i> [67]	0.7790	0.0591	0.9240	Multiscale
Hoover <i>et al.</i> [2]	0.6751	0.0433	0.9267	Matched filter
Xiaoyi and Mojon [44]	—	—	0.9337	Matched filter
Yao and Chen [71]	0.8035	0.0280	—	Matched filter
Zhang <i>et al.</i> [47]	0.7177	0.0247	0.9484	Matched filter

2.3 Medical image registration: A review

Digital image processing is applied on medical images and these images are used for diagnosis, disease monitoring, treatment planning and guidance for surgery. A large variety of medical imaging modalities exist that have been used as primary inputs for medical image registration studies. The selection of the imaging modality for a clinical study requires medical insights specific to organs considered. It is impossible to capture all the details from one imaging modality that would ensure clinical accuracy and robustness of the analysis and resulting diagnosis. Some of the major modalities in clinical practice include Computerized Tomography (CT), Computerized Tomography used for Angiography (CTA), Quantitative Computed Tomography (QCT), Quantitative Coronary Angiography (QCA), Quantitative Vascular Angiography (QVA), Hip Structural Analy-

sis (HSA), Magnetic Resonance Imaging (MRI), Magnetic Resonance imaging used for Angiography (MRA), Dynamic Contrast-Enhanced Magnetic Resonance Imaging (DCE-MRI), nuclear medicine using Multi-Gated Acquisition scan (MUGA), Single Photon Emission Computed Tomography (SPECT), Positron Emission Tomography (PET), ultrasound for abdominal/small parts ultrasound, echo- cardiograph, Intimal-Media Thickness (IMT), Contrast Enhanced UltraSound (CEUS), X-ray imaging for mammography. These imaging modalities find a large range of application in diagnosis and assessment of medical conditions affecting brain, breast, bone marrow, abdomen (liver, kidney and spleen), cervical, chest, lung, entire body, pelvis, prostate, whole thorax , mouth, teeth, retina, intestines and soft tissues. The images obtained by using different imaging modalities needs to be compared with the one another and combined for analysis and decision making. For disease progress monitoring and growth of abnormal structures, images are acquired at different times and stages, different depths or with different modalities. The misalignment between images are inevitable and reduces the accuracy of further analysis. To deal with these issues image registration process plays an important role in medical image analysis and provides a platform for group analysis and statistical parametric mapping.

The registration is the process to determine a geometrical transformation that align points in one view of an image with corresponding points in another view of that image or other image. The other medical applications of medical image registration systems include:

- Monitoring of healing therapy and tumor evolution.
- Combination of sensors recorded anatomical body structure like MRI, CT with sensors monitoring functional and metabolic activities like PET, SPECT etc.
- Comparison of patient's image with digital anatomical atlases and specimen classification.
- Characterizing normal versus abnormal anatomical shape variations.

- Identify the changes in retinal blood vessel structure for better pathology detection etc.

In addition to medical application of a registration system, the other application areas where it is used are astrophysics (alignment of images from different frequencies), military applications (target recognition), remote sensing, and many others. A good overview of these applications of image registration is presented in [72]. Any registration technique can be described with the help of four components that are the feature space, the search space, the search strategy and the similarity metric [73]. The feature space, where features to be matched are selected in the image pair and the range of transformation or the search space relates the source and target images. To find the optimum transformation within the search space using an optimization algorithm, the similarity metric is used to measure the similarity between source and target image which determines the optimal transformation parameters to be used as a function of the similarity measure. Because of its importance the topic of medical image registration is useful for both researchers and medical practitioners.

If we go through the literature survey on medical image registration then it is found that various author works on that, for example Maintz and Vierger [72] had suggested the nine fundamental criterion to classify the various methodologies used for medical image registration that is dimensionality, nature of registration basis, nature of transformation, domain of transformation, degree of interaction, optimization procedure, modalities involved, subject and object. In papers [74], [75], authors suggested the two classification criteria of the image registration techniques a multi-modal registration and temporal registration, where the multi-modal registration handles the registration of images of the same scene acquired from different sensors e.g. integrate structural information from CT or MRI with functional information from radio nucleic scanners such as PET or SPECT for anatomically locating metabolic function. Where as the temporal registration can handles the registration of images of the same scene taken at different times or under different conditions e.g. digital subtraction angiography registration of images before and after radio isotope injections to characterize functionality, digital subtraction mammography to

detect tumors etc. In paper [76], authors presented a review of deformable medical image registration system and discussed about deformable registration methods with emphasis on the recent advances in the domain of multi-modality fusion, longitudinal studies, population modeling, and statistical atlases. Francisco *et al.* [77] presented a review of medical image registration system and classify the medical image registration system into intensity based and feature based, where the author explored different methodologies used for the design of the intensity and feature based medical image registration system. In literature many authors presented the methodologies for the design and development of medical image registration system for specific imaging modalities. M. Essadiki presented a technique for combining panchromatic and multi-spectral spot images [78]. Flusser used moment based approach to correct affine distortion and they had done medical image analysis for degraded images to locate invariants [79]. J.P.W. Plum presented multi-modal image registration using generalized survival exponential entropy medical image computing [80]. E.A. Sascha *et al.* [81] proposed a DIRBoost algorithm which is inspired by the theory on hypothesis boosting which is the well known field of machine learning. Many authors presented their work on medical image registration according to various applications in hand such as cardiac applications [82], nuclear medicine [83], radiation therapy [84], digital subtraction angiography [85], and brain warping applications [86]. In papers [87], [88] author focused on modeling of soft-tissue deformation during imaging or surgery and papers [89], [90], [91] present the model changes in anatomy of the object of interest.

2.3.1 Retinal image registration

In this thesis, our concentration is to present a literature survey on retinal image registration and describes the advantages and limitations of the existing methods which may be used in real time applications.

In 1995 article published by the author Cideciyan *et al.* [92] which describe a digital image registration algorithm based on the cross correlation of triple invariant image descriptors. This algorithm is applied to ocular fundus images, and its accuracy and reliability are quantified using simulated transformations, simulated noise, and a series of

actual fundus images.

The ocular fundus refers to the inside back portion of the eye, including the retina. Imaging of the ocular fundus is a non-invasive technique to diagnose and document various eye diseases and their progression over time. Ophthalmologists commonly compare fundus images with overlapping content, a task that requires careful visual inspection. The reason behind that fundus photographs imaging the same retinal area in the same eye are usually misaligned. The misalignment is due to changes in the geometry between fundus and camera. The decision of the expert on the relationship between the images of interest may be significantly accelerated and improved if a computer enables automated superimposition of two images. But the manipulation of images so that the information contents are superimposable is a very difficult computational problem.

Registration is the solution to this problem; it aims at transforming the images of interest such that they appear to have been recorded without change in geometry between fundus and camera. This article demonstrated the application of the cross-correlation based registration algorithm for the alignment of fundus images differing in translation, rotation angle, and uniform scale factor. It was shown that in the case of simulated transformations and simulated noise, the algorithm is extremely accurate and robust.

In 2003 paper published by the author Stewart *et al.* [93] introduces and analyzes a new registration algorithm called Dual-Bootstrap Iterative Closest Point (Dual-Bootstrap ICP). The approach is to start from one or more initial, low-order estimates that are only accurate in small image regions, called bootstrap regions. In each bootstrap region, the algorithm iteratively executes the steps, refines the transformation estimate, expands the bootstrap region and tests to see if a higher order transformation model can be used until the region expands to cover the overlap between images. The step expands the bootstrap region and test is governed by the covariance matrix of the estimated transformation. The step refines the transformation estimate uses a novel robust version of the ICP algorithm.

In registering retinal image pairs, Dual-Bootstrap ICP is initialized by automatically matching individual vascular landmarks, and it aligns images based on detected blood vessel centerlines. The author introduced the Dual-Bootstrap ICP algorithm and success-

fully applied it to retinal image registration. The idea behind the algorithm is to start from an initial estimate that is only assumed to be accurate over a small region.

The advantages of the Dual-Bootstrap ICP algorithm in as follows:

- In comparison with current indexing-based initialization methods and minimal-subset random sampling methods, Dual-Bootstrap ICP has the major advantage. It requires fewer initial correspondences.
- In comparison with multi resolution methods, Dual-Bootstrap ICP starts from what might be thought of as a keyhole view on the alignment rather than the bird's-eye view of multi resolution.
- Instead of matching globally, which could require simultaneous consideration of multiple matches [92], Dual-Bootstrap ICP uses region and model bootstrapping to resolve matching ambiguities.
- This is especially important when there is no clear relationship between features in the two images.

The disadvantages of the Dual-Bootstrap ICP algorithm:- It can fails in two ways.

- When the initial model is too weak.
- When the images contain two geometrically separated clusters of features, and the initial transformation is estimated only in a single cluster.

According to the author developing a robust, low-contrast feature extraction is main focus to further improvements in retinal image registration.

In 2004 paper published by the author Fischer *et al.* [94] propose a novel registration technique, which combines the concepts of landmark and automatic, non-rigid intensity based approaches. This novel approach enables the incorporation of different distance measures as well as different smoothers. The proposed scheme does minimize a regularized distance measure subject to some interpolation constraints. The desired deformation is computed iteratively using an Euler-scheme for the first variation of the chosen objective functional.

This scheme is fast and robust numerical scheme for the computation of the wanted minimizer development, implementation and applied to various registration tasks. It also includes the registration of pre- and post intervention images of human eye. This framework is parameter-free, non-rigid registration scheme which allows for the additional incorporation of user defined landmarks is proposed. It enhances the reliability of conventional approaches considerably and acceptability.

In 2004 paper published by the author Matsopoulos *et al.* [95] proposed an automatic method for registering multi modal retinal images. The method consists of three steps:

- Vessel centerline detection and extraction of bifurcation points only in the source image.
- Automatic correspondence of bifurcation points in the two images using a novel implementation of the self organizing maps.
- Extraction of the parameters of the affine transform using the previously obtained correspondences.

In this paper author introduce two novel implementations that are as follows:

- The application of the vessel centerline detection and bifurcations extraction process only on the reference image. This step simplifies the registration methodology since candidate points are identified only on the reference image.
- The novel implementation of the Self Organizing Map (SOM) network to define automatic correspondence of the bifurcation points between the reference and target image.

The SOM is a neural network algorithm, which uses a competitive learning technique to train itself in an unsupervised manner. Kohonen first established the relevant theory and explored possible applications [96].

In 2008 paper published by the author Lin Y *et al.* [97] propose a 2D registration method for multi modal image sequences of the retinal fundus, and a 3D metric reconstruction of near planar surface from multiple views. There are two major contributions in this paper first one is for 2D and second is for 3D registration.

For 2D registration, this method produces high registration rates while accounting for large modality differences. In Comparison with the state of the art method [98], it was found that this approach required less computation time. This is achieved by extracting features from the edge maps of the contrast enhanced images, and performing pairwise registration by matching the features in an iterative manner, maximizing the number of matches and estimating homographs accurately. For 3D registration part, images are registered to the reference frame by transforming points via a reconstructed 3D surface. The author contribution is the proposed 4-Pass Bundle Adjustment (4P-BA) method that gives optimal estimation of all camera poses. With accurate camera poses, the 3D surface can be reconstructed using the images associated with the cameras with the largest baseline. Compared with state of the art on 3D retinal image registration methods, it was found that this approach produces better results in all image sets.

In 2D registration method that register multi-modality images accurately with high registration rate and a 3D surface reconstruction method that recovers accurate camera poses and 3D structure for 3D registration. In 2D registration, SIFT features are extracted from edge maps and iteratively matched to produce a larger set of reliable matches from which an accurate homograph can be estimated. In 3D registration, author use 4P-BA to recover accurate camera poses, which gives the clue to select the best image associated with the camera with the largest baseline. According to the author in future includes validating this approach on a larger data set, increasing the 3D registration rate, and 3D surface reconstruction from multiple views.

In 2010 paper published by the author Tsai *et al.* [99] proposed an Edge-Driven DB-ICP, targeting the least reliable component of GDB-ICP, modifies generation of key point matches for initialization by extracting the Lowe key points from the gradient magnitude image and enriching the key point descriptor with global-shape context using the edge points. The ultimate goal of this algorithm is to designed jointly align in a common reference space and all the images in a complete Fluorescein Angiogram (FA) sequence, which contains both red-free (RF) and FA images.

This work is inspired by Dual-Bootstrap Iterative Closest Point (DB-ICP), which rank-

orders Lowe key point matches and refines the transformation, going from local and low-order to global and higher-order model, computed from each key point match in succession. There are two major challenges in solving the registration problems of a complete FA sequence are as follows:

- Various parts of the vasculature are nonlinear intensity related in both local and global scales between multi modal pairs, as well as FA image pairs of different phases.
- Various parts of the vasculature are nonlinear intensity related in both local and global scales between multi modal pairs, as well as FA image pairs of different phases.

So this proposed method addresses the above two challenges by exploiting the structural similarity between two images in order to increase the robustness of the pairwise registration, which in turn improves the completeness of the joint registration for the image sequence. The main contribution of author is two-fold. First, they propose a new key point extraction and matching algorithm to robustly generate initial transformations. Second, building heavily on existing techniques, where they present an end-to-end automatic registration system tailored for multi modal image registration for a complete FA sequence.

2.3.2 Feature based retinal image registration

Retinal images registration is a challenging task [100] due to following reasons.

- The retina is a curved surface; nonlinear deformation may occur when using a weak-perspective uncalibrated camera.
- Image overlap may be small due to large viewpoint change between images.
- Retinal images may have large texture-less regions with uneven illumination which make the extraction of retinal vessels very difficult.
- Two images taken long time apart or from diseased eyes can have physical changes in both structure and color of the retina.

In the past twenty years, many techniques have been proposed to solve the retinal image registration problem in different ways. Generally, these methods can be classified into two main categories: vessel-based and non vessel-based methods. The non vessel-based methods cannot use the retinal blood vessel directly during image registration. These methods are further divided into two categories: intensity-based and image descriptor-based methods.

The intensity-based retinal image registration techniques usually rely on image intensities and gradients, the registration is carried out through optimizing and certain similarity measures, such as mutual information [101], and cross-correlation of images. Various optimization methods can be used for finding global optimum of the cost function, including downhill simplex, simulated annealing [101], [102], genetic algorithms [102], and so forth. An author J.C. Nunes *et al.* [103] was proposed, a multi scale elastic registration scheme to take into account retinal intensity variants based on optical flows. The main limitations of intensity-based methods lie in two aspects:

- These techniques are highly reliant on the consistent intensities in two images and tend to fail due to the presence of nonuniform illumination and large texture less regions.
- The optimization may have huge searching space so that the computational cost becomes a high for intensity-based techniques to be applied in clinic.

The descriptor-based retinal image registration techniques [99], [104], [105] are feature-based and become popular recently. Instead of optimizing a similarity function with whole image intensities, these methods extract local invariant descriptors as image features. Hence, image registration is equivalent to finding correspondences between two feature sets. The author G. Yang *et al.* [104] was proposed a Generalized Dual-Bootstrap Iterative Closest Point (GDB-ICP) where SIFT local descriptor is used and the alignment process is driven by two types of key points: a corner points and bifurcation points. An author Tsai *et al.* [99], was proposed an edge-driven DB-ICP algorithm by enriching the key point descriptor with shape context using edge points to deal the multi-modal registration problem. Further an author J. Zheng *et al.* [105] was proposed a new salient

feature region descriptor based approach for poor quality retinal images registration.

The vessel-based techniques utilize the retinal vascular features as a basis for image matching. Currently, most of the retinal image registration approaches are vessel-based [100], [22], [106], [107], [93], [95], [108], because the retinal vessels are the most prominent representation for retina. In general, the vessel-based techniques consist of two independent steps: vessel segmentation and vascular feature-based registration. The author Stewart *et al.* [93] have proposed, a dual-bootstrap iterative closest point (DB-ICP) algorithm to match vascular centerlines. It started with some initial low-order estimations and iteratively refined the results by expanding the bootstrap regions with higher-order transformation model. Further, in order to make the matching robust to mismatches between feature points, hierarchical transformation models were employed in [100]. The author *et al.* [106] was proposed, a hybrid retinal image registration approach by combining both intensity-based and vessel-based methods. To achieve both global and local alignments, an elastic matching scheme is used in [107] based on reconstructed vascular trees. Usually, the vessel-based method are supposed to be more reliable than non vessel-based method because the vascular features are sufficient (but not too many) and accurate as landmarks and preferable spread over whole image region. The main drawback of vessel-based methods is the local convergence problem when initial misalignment is large and mass of segmentation noises exist. The performance of feature based segmented retinal image registration approach is evaluated by using the Normalized Cross Correlation (NCC) which is commonly used similarity measure between two registered images [109], [110]. There are some other similarity measures are exist in literature which is describe in section 2.7.

2.4 Performance measures

2.4.1 Performance measures for segmentation

The performance of retinal blood vessel segmentation approach is measured on the basis of pixel-by-pixel classification result. Any pixel is classified either as a vessel or not.

Consequently, there are four possibilities; two classifications and two misclassifications. The two classifications are True Positive (TP), and True Negative (TN) which is defined as follows:

- The pixel is True Positive (TP) when a pixel is identified as vessel in both the ground truth and segmented image.
- The pixel is True Negative (TN) when a pixel is classified as a non-vessel in the both the ground truth and the segmented image.

The two misclassifications are False Positive (FP), and False Negative (FN) which is defined as follows:

- the pixel is False Positive (FP) when a pixel is classified as vessel in the segmented image but non-vessel in the ground truth image.
- The pixel is False Negative (FN) when a pixel is classified as non-vessel in the segmented image but as a vessel pixel in the ground truth image.

On the basis of TP, TN, FP, FN calculate performance measures, the True Positive Rate (TPR), False Positive Rate (FPR), and Accuracy (Acc). The True Positive Rate (TPR) is also known as sensitivity, represents the fraction of pixels correctly detected as vessel pixels.

$$TPR = \frac{TP}{TP + FN} \quad (2.1)$$

The False Positive Rate (FPR) is the fraction of pixels erroneously detected as vessel pixels.

$$FPR = \frac{FP}{TN + FP} \quad (2.2)$$

The Accuracy (Acc) is measured by the ratio of the total number of correctly classified pixels (sum of true positives and true negatives) to the number of pixels in the image field of view. The accuracy of the segmentation approach is evaluated by using following equation:

$$Accuracy = \frac{TP + TN}{TP + TN + FP + FN} \quad (2.3)$$

Sensitivity reflects the ability of the algorithm to detect the vessel pixels. Specificity (SP) is the ability to detect non vessel pixels. It can be expressed as $(1 - \text{FPR})$.

A Receiver Operating Characteristic (ROC) curve plots the fraction of vessel pixels correctly classified as vessel, namely the TPR, versus the fraction of non-vessel pixels wrongly classified as vessel, namely the FPR. The closer the curve approaches the top left corner; the better is the performance of the system. The most frequently used performance measure extracted from the ROC curve is the value of the Area Under the Curve (AUC) which is 1 for an optimal system. For retinal images, the TPR and FPR are computed considering only pixels inside the field of view.

2.4.2 Performance measures for registration

Similarity measure is most widely used registration basis for many applications. The intensity is referring as the scalar values of image pixels. The pixel value depends on the modality involve in the registration process. In case of intensity-base registration the transformation process is based on the pixel intensity and it is determined by iteratively optimizing the similarity measure calculated from all pixel values. In case of poor pixel value the optimization is not able to provide better result so refer the similarity measure as a voxel similarity measure. But the running time complexity of registration algorithm is high when uses all voxel in similarity measure so in practice, generally use a subset of voxel and for that a little bit preprocessing are required. The subset of voxel is either selected randomly or by using regular grid. In some algorithms the voxels are selected from defined Region of Interest (ROI), so the pre-segmentation of the images are required. This preprocessing depends on the modality of medical images and body parts which is being studied. Sometimes the intensity based similarity measures are applied on the derived parameter such as image gradients of the image rather than the voxel values [111].

There are various types of similarity measures that are used in intensity and feature based image registration methods as shown in Figure 2.1. Before describing the similarity measures, let us consider the images to be registered are source image I_s and target image I_t , the set of voxel of these images are $I_s(i)$ and $I_t(i)$ respectively. Image I_t is iteratively

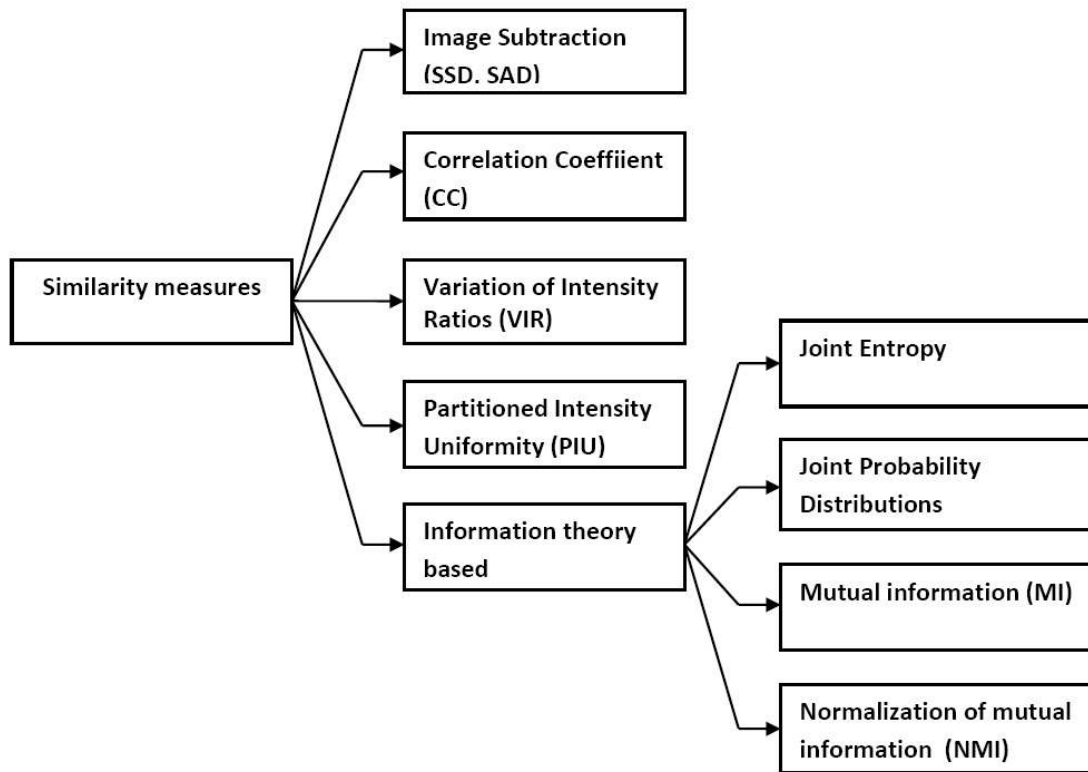


Figure 2.1: Type of Similarity Measures

transformed to $I_t(T)$ by successively apply transformation T i.e. $I_t(T) = T(I_t)$.

2.4.2.1 Sum of squares differences

Sum of Squares Differences (SSD) is a similarity measure also known as image subtraction and used to identify the alignment of images I_s and I_t . When the value of SSD is zero then both images are aligned correctly otherwise there are some misalignment. The misalignment is directly proportional to the increasing value of SSD. The SSD is the optimum measure when two images only differ by Gaussian noise [112]. Normally SSD is work well, when all used images in registration process are nearly identical except for small change. For example this approach was used in serial registration of MR images and fMRI experiments [113], [114]. SSD is used by Friston's Statistical Parametric Mapping software (SPM), which is based on a linear approximation [115], [116]. The SSD is sensitive when small set of voxels having very large intensity differences between images

I_s and I_t . The effect of these outliers voxels cannot be reduced by SSD, so the Sum of Absolute Difference (SAD) can be used to reduce the effect of outliers [117]. SSD and SAD are calculated by using Eq^n-1 and Eq^n-2 respectively as show in Table 2.3.

2.4.2.2 Correlation Coefficient

The Correlation Coefficient (CC) is used as similarity measure, where the intensities of images I_s and I_t are linearly related [112]. For example ultrasound image features of the wrist are linearly related to finger positions [118] and supine magnetic resonance imaging Cobb measurements or idiopathic scoliosis are linearly related to measurement from standing plain radio-graphs [119]. The main characteristic of correlation techniques is carried out the correlation in either the spatial domain or the spatial frequency domain (k-space) [117]. K-space is widely used in magnetic resonance imaging first introduced by Likes in 1979 and then by Ljunggren and Twieg in 1983. According to the MRI physics, k-space is use in 2-D or 3-D Fourier transform of the MR image and having complex values that are sampled during an MR measurement, in a premeditated scheme controlled by a pulse sequence, i.e. an accurately timed sequence of radio frequency and gradient pulses [120], [121]. This type of approach has been applied on medical images, but the applicability appears to be limited by the implicit assumption that the objects of interest are in the fields of view of both images being registered [122], [123]. The CC is calculate by using Eq^n-3 as show in Table 2.3.

2.4.2.3 Variance of Intensity Ratio

The Variance of Intensity Ratio (VIR) is also known as Ratio-Image Uniformity (RIU). It is widely used in intra-modality registration that means, it is apply for same image modality. The VIR algorithm was initially proposed by Woods for the registration of serial PET images in 1992 [124] and then used for serial MR image registration in 1998 [125]. This algorithm is working with a derived image ratio which is calculated by dividing the each pixel of image I_s by each pixel in transform image I_t' . To find the transformation iteratively that maximized the uniformity of the image ratio, determined by calculating

the normalized standard deviation of image ratio. The uniformity of the image ratio is inversely proportional to the normalized standard deviation of image ratio [111], [117]. The VIR is calculate by using Eq^n-4 as show in Table 2.3.

2.4.2.4 Partitioned Intensity Uniformity

The Partitioned Intensity Uniformity (PIU) is widely used for inter-modality registration that means apply for different modality of image. Wood proposed the modified version of own VIR algorithm for MR-PET registration, which is known as PIU [126]. The PIU algorithm use an idealized assumption, that is "all pixels with a particular MR pixel value represent the same tissue type so that values of corresponding PET pixels should also be similar to each other" [111]. The PIU algorithm partition the PET image into 256 separate groups or iso-intensity sets, which is based on the values of PET image voxels then maximize the uniformity of the MR voxel values within each groups. After that uniformity is maximized within each group by minimizing the normalized standard deviation. The PIU have two different versions depending on whether image MR or image PET is partitioned [117]. The PIR is calculate by using Eq^n-5 as show in Table 2.3.

2.4.2.5 Information Theory based Similarity Measures

There are various types of similarity measures techniques based on information theory like joint histogram and joint probability distribution, joint entropy, Mutual Information (MI). The Shannon-Wiener entropy measure (S_e) is commonly used technique for measure of information in signal and image processing [127], [128]. The Shannon-Wiener entropy (S_e) is measure by using a formula as show in Eq^n-6 , Table 2.3 and is derived from three conditions that are able to measure the uncertainty in a communication channel. First the S_e should be continuous in p_i , second if all p_i equal to $\frac{1}{n}$ then S_e should be monotonically increasing in n, where n is number of symbols. For example if there are two images used in image registration then there are two symbols at each voxel location then value of n is equals to two and the last condition, if a choice is broken into sequence of choices then the S_e should be the weighted sum of the constituent S_e . Shannon proved

that S_e is unique formula which satisfies all these three conditions. The entropy having minimum value of zero when the probability of occurring (p_i) one symbol is one and other is zero and the entropy will be maximum if all symbols having equal probability of occurrence [111].

A joint histogram is useful for visualizing the relationship between the intensity of corresponding voxel in two or more image. Joint histograms also consider many features such as edge, density, gradient magnitude and rank. It is generally used in multi spectral data and becomes n-dimensional when n number of images used to generate it. For two images I_s and I_t the joint histogram is two dimensional and it is constructed by plotting the intensity $I_s(i)$ of each voxel in image I_s against the intensity $I_t(i)$ of each voxel in image I_t . So the axes of histogram are the intensities or intensity partitions in each image. The value at each point in the histogram is the number of corresponding voxel pairs with a particular combination of intensities in the different spectral components. [129]. If the joint histogram is normalized, then it is use for the estimation of the joint probability distribution function (pdf) of intensities in the images [130].

Mutual information as a registration measure is introduce in 1990 by Woods *et al.* [124], [126] to defining the regions of similar tissue in between the different modality of images. According to the book chapter [131], [132] mutual information(MI) in the form of conditional entropy is defined for two images I_s and I_t by Eq^n-8 , Table 2.3 and defined in the form of joint entropy by Eq^n-9 , Table 2.3. The MI has similar interpretation to the joint entropy. Both metrics reflect how much information of one image has about another. Many researchers used MI based similarity measure rather than joint entropy based similarity measure for image registration because MI is avoid favoring a transformation that forces the image so far apart that only background is contained in the overlap region. According to the formula for joint entropy Eq^n-7 , Table 2.3, the joint entropy is minimized at two points, when $S_e(I_s)$ is small and I_t is dependent on I_s but in case of maximizing the MI by maximize $S_e(I_s)$, while at same time limiting $S_e(I_s|I_t)$, where $S_e(I_s|I_t)$ is joint Shannon's entropy of the joint probability histogram. The maximal entropy of $S_e(I_s)$ ensures that the overlap region between two images contains most of the images, including complex parts

that increase individual entropy [133], [134].

MI is provide some improvement to solve the overlap problem but it is fail for some type of clinical image that contains a large amount of noise or air around the outside of the subject that means changes in overlap of very low intensity regions of the image can disproportionately contribute to the mutual information. Alternative option to improve the performance of mutual information is normalization schemes. There are some schemes for normalization of MI (NMI) have been proposed in journal articles [135], [136]. The Studholme *et al.* [136] proposed a method for normalization of MI that overcome the sensitivity of mutual information to change in image overlap and NMI is calculated by using Eq^n -10, Table 2.3.

Table 2.3: Equation used for different similarity measure

Similarity measure	Formula	Eq ⁿ
SSD	$\text{SSD} = \frac{1}{N} \sum_i^N I_s(i) - I_t(i) ^2$ <p>where $\forall i \in I_s \cap I_t$</p>	(1)
SAD	$\text{SAD} = \frac{1}{N} \sum_i I_s(i) - I_t(i) $ <p>where $\forall i \in I_s \cap I_t$</p>	(2)
CC	$\text{CC} = \frac{\sum_i (I_s(i) - \bar{I}_s) (I_t(i) - \bar{I}_t)}{\{\sum_i (I_s(i) - \bar{I}_s)^2 \sum_i (I_t(i) - \bar{I}_t)^2\}^{1/2}}$	(3)
VIR	$\text{VIR} = \frac{\sigma_R}{\mu_R}$ <p>where $\sigma_R = \frac{1}{N} \sum_i (R(i) - \mu_R)^2$</p> $\mu_R = \frac{1}{N} \sum_i R(i)$ <p>and $R(i) = I_t(i)/I_s(i)$</p>	(4)
PIU	$\text{PIU} = \sum_{a \in \{a\}} \frac{n_s(a)}{N} \frac{\sigma_t(a)}{\mu_t(a)}$ <p>where $s \equiv I_s$ and $t' \equiv I_t'$</p> <p>$n_s(a)$ is the number of voxels in image s and a is partition in image s</p>	(5)
SE	$S_e = - \sum_i p_i \log p_i$	(6)
JSE	$JS_e(I_s, I_t) = S_e(I_s) + S_e(I_t I_s)$	(7)
MI	<p>MI in the form of conditional entropy</p> $\text{MI}(I_s, I_t) = S_e(I_s) - S_e(I_s I_t)$	(8)
MI	<p>MI in the form of joint entropy</p> $\text{MI}(I_s, I_t) = S_e(I_s) + S_e(I_t) - S_e(I_s, I_t)$	(9)
NMI	$\text{NMI}(I_s, I_t) = \frac{S_e(I_s) + S_e(I_t)}{S_e(I_s, I_t)}$	(10)

2.5 Database used for retinal blood vessels Segmentation

Mostly the DRIVE and STARE databases are used to evaluate the performance of various retinal blood vessel segmentation approaches.

2.5.1 DRIVE Database

The DRIVE (Digital Retinal Images for Vessel Extraction) database is freely available on-line [2]. The images taken from the DRIVE database were obtained from a diabetic retinopathy screening program in the Netherlands [137]. The screening population consisted of 400 images of diabetic subjects between 25 to 90 years of age and forty images have been randomly selected. Out of 40 images, 33 do not contain any diabetic retinopathy and 7 show a mild early diabetic retinopathy [26]. The healthy and diabetic retinopathy retinal images taken from the DRIVE database are shown in Figure 2.2(a) and (b) respectively. The images of the DRIVE database were acquired from Canon CR5 non-mydratic 3CCD camera with a 45 degree field of view (FOV). The captured images contain 8 bits per color plane at 768×584 pixels. The ground truth image was manually segmented and segmentation process was performed by observers, a computer science student, and they have been trained by an experienced ophthalmologist Michael D. Abramoff and [26]. The ground truth images of color retinal images as shown in Figure 2.2(a) and (b) are given in Figure 2.2(c) and (d) respectively. These 40 images were divided into two sets a test set and a training set and each set contains 20 original retinal images together with respective ground truth images. Mostly the performance of retinal blood vessel segmentation approaches is measured on the test set.

2.5.2 STARE Database

Images of STARE (STructured Analysis of the Retina) database were obtained from the Shiley Eye Center at the University of California, which is on-line freely available [2]. These images were captured by a TopCon TRV-50 fundus camera at 35 degree field of view. The captured images contain 8 bits per color channel at 650×500 pixels. The

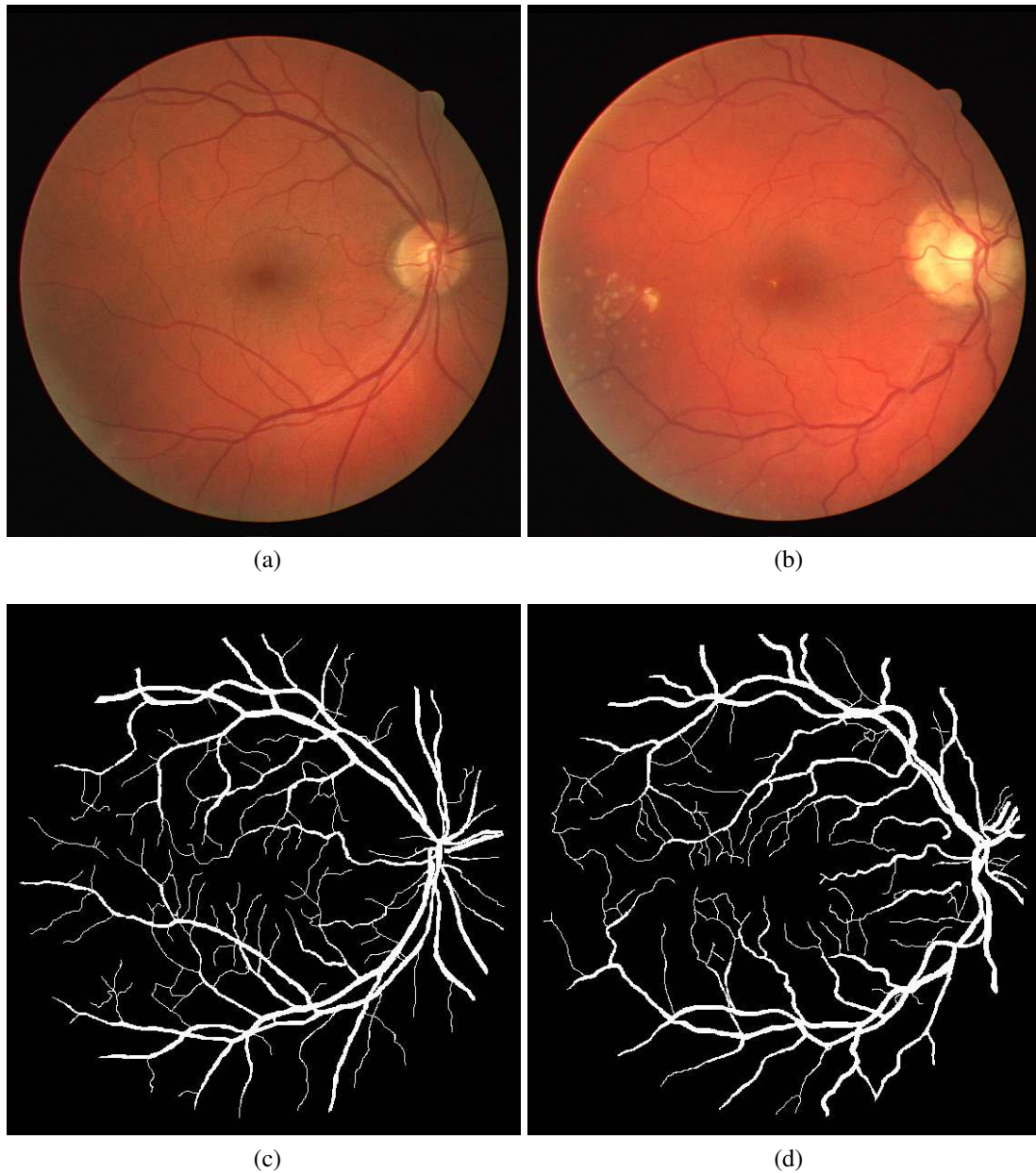


Figure 2.2: The image taken from DRIVE database: (a) Healthy retinal image (b) diabetic retinopathy infected retinal image and (c), (d) are the respective segmented ground truth retinal images

STARE database contains 20 retinal images and out of 20 images there are 10 healthy retinal fundus images and the remaining belong to unhealthy retinal images. The ground truth image was manually segmented and segmentation process was performed by two observers namely Adam Hoover and Valentina Kouznetsova. The healthy and pathology infected retinal images taken from STARE database are shown in Figure 2.3(a) and (b) respectively, and their respective ground truth images are shown in Figure 2.3(c) and (d).

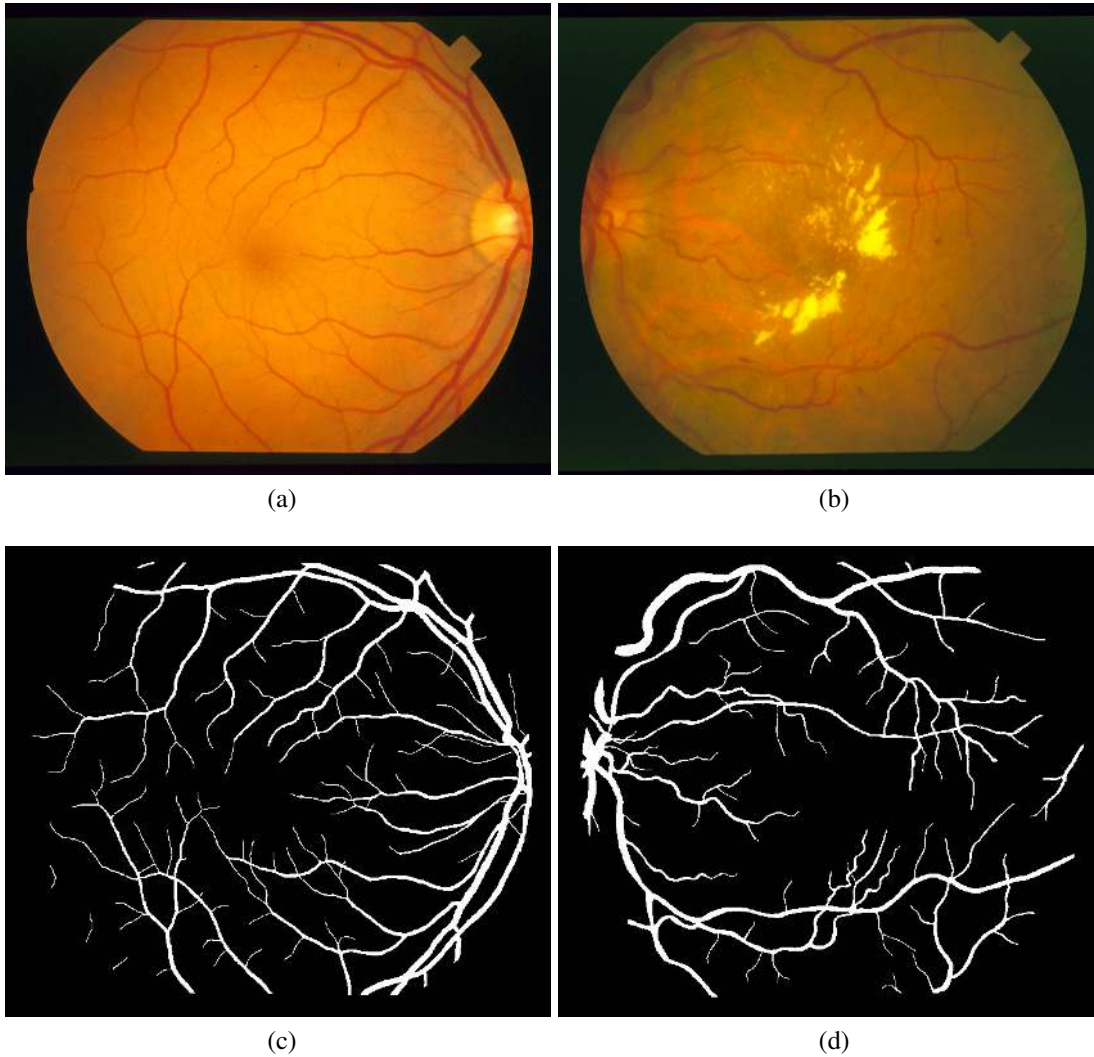


Figure 2.3: The image taken from STARE database: (a) Healthy retinal image (b) pathology infected retinal image and (c), (d) are the respective segmented ground truth retinal images

2.6 Discussion

The objectives of the present discussion is to analyze the various matched filter based retinal blood vessel segmentation approaches, feature based segmented retinal image registration, and similarity measure presented in this survey.

First, start the discussion about the retinal blood vessel segmentation approach. In general the performance of retinal blood vessels segmentation approach based on supervised classification is better than their counterparts. Almost all the supervised methods report the accuracy approximately 0.95 and among them Lupascu *et al.* [50] and Marin

et al. [53] reported the highest for DRIVE and STARE database respectively. However, these methods do not work very well on the images with non uniform illumination as they produce false detection in various images on the border of the optic disc, hemorrhages and other types of pathologies that present strong contrast.

The matched filter based approach has been extensively used for automated retinal vessel segmentation [6]. The matched filter based approaches use the prior knowledge about the shape and symmetry of the cross-section profile of the retinal blood vessel with respect to their location and scale parameter. Many improvements and modifications are proposed after the introducing the Gaussian matched filter by Chaudhuri *et al.* [12]. Various authors improved the performance of matched filter based approach by improving the thresholding techniques [138, 44] rather than changing the Gaussian shaped matched filter kernel. First time author H. Zolfagharnasa *et al.* [14] replaced the Gaussian function based matched filter by Cauchy probability density function (pdf) and reported that the accuracy of retinal blood vessel detection was substantially improved. Therefore in this thesis we try to improve the performance of matched filter base retinal blood vessels segmentation approach by selecting the suitable probability density function that matched better with the cross-sectional intensity profile of retinal image.

Secondly, start the discussion about the registration techniques for retinal image. The non vessel-based registration technique which is divided in two parts intensity-based and descriptor-based. some authors are working on intensity-based [101], [102], [103] but this technique is not much useful for retinal image registration. Reason behind that it fails in the presence of nonuniform illumination and large texture less region. It also required much computational time because it may have required huge searching space during optimization. whereas descriptor-based or feature based techniques become popular recently. Because in this technique, instead of optimizing a similarity function with whole image intensities, these methods extract local invariant descriptors as image features. In comparison with intensity-based the feature based technique become more suitable for retinal image registration.

When we compare the feature-based registration technique with vessel-based then it

is found that the authors may use either feature-based or vessel-based registration techniques because in both cases, the vascular features are sufficient and accurate as landmarks and preferable spread over the whole image region. In comparison to the vessel-based, the feature-based technique is more suitable for retinal image registration because the vessel-based method has a local convergence problem when initial misalignment is large and mass of segmentation noises exist. Therefore, in this thesis we use the feature based retinal image registration technique.

The next component of the discussion is the similarity measures used to identify the alignment of the images. The similarity measures based on the intensity difference (SSD, SAD, MSD etc.) are computed from the voxel intensity of the corresponding structures of both images so lower SSD indicates better alignment. The CC and its related similarity measures are based on the assumption that there is a linear relationship between the intensities of the corresponding structure of both images so larger CC indicates better alignment. The SSD, SAD, CC and its derived similarity measures are most appropriate for mono-modal image registration and these measures are based on voxel to voxel stationarity of the intensities and inaccuracy of independence. The VIR and PIU similarity measures are appropriate for serial intra-modality and inter-modality image registration respectively. The VIR method maximizes uniformity by minimizing the normalized standard deviation. In some cases it gives good result, but preprocessing is required that remove some anatomy. The PIU is an improved version of VIR, which overcome these problems. The VIR and PIU can be useful for both the intensity based as well as feature based registration, whereas the information theory based similarity measures are appropriate for intensity based image registration and applied for both intra-modality as well as inter-modality image registration and provide maximum value when the input images are registered correctly. The SSD, CC, VIR and PIU are the distance based and the information theory based are based on probabilistic approaches. Generally, distance based approaches can be used in feature based image registration, whereas the probabilistic approach based similarity measure is useful in intensity-based image registration.

In comparison with CC and its derived similarity measure the MI has a big advantage

because it is able for accurate registration of multi modal images and also able to measure the alignment of image signals which is helpful to predict the other but CC fails for the same. If how to transform one image signals to another is known then it is simple to apply that transformation and then correlation performs well on the normalized image signals. The joint entropy based similarity measures has some advantages over PIU such as it minimizes the spread of clusters in two dimensions rather than one and minimizing entropy does not require that the histograms are uni-modal in the way to minimizing variance. So the joint entropy would be normally applicable to multi-modality registration. In case of feature based segmented retinal image registration, the CC and NCC are suitable similarity measure. Reason behind that variation of intensity level between the retinal blood vessel and their background is low. Another reason, the segmented retinal image registration generally belong to the category of mono model image registration.

2.7 Conclusion

In this chapter a comprehensive literature survey of methodologies involved in retinal blood vessel segmentation, retinal image registration, including a short summary of medical image registration and the similarity measures used for medical as well as retinal image segmentation and registration. This chapter also includes a definitive documentation on theoretical aspects together with the merits and limitations of different methodologies used for retinal image segmentation and registration. After comprehensive literature analysis on theoretical aspects we found the following outcomes:

- The matched filter based retinal blood vessel segmentation approach is better with respect to other segmentation approaches as reported in the literature.
- The descriptor-based or feature base registration technique is suitable for segmented retinal image registration with respect to other registration techniques as reported in the literature.
- To identify the performance of the retinal image registration approach, the CC or NCC are suitable similarity measure.